PAPER

Check for updates

On-chip colorimetric assay for determining serum lithium concentration from whole blood†

Carl Olsson, [a] Janosch Hauser, [a] Federico Ribet, [a] Fredrik Wikström,[bcd] André Görgens, [efg] Olof Beck, [h] Martin Schalling, [bd] Lena Backlund [bd] and Niclas Roxhed [*ai]

Lithium is the first-line treatment for bipolar disorder. However, the narrow therapeutic window of serum (s-)lithium is near its toxicity range, necessitating continuous monitoring of patients, a process involving regular hospital visits. On-demand home sampling could allow for more frequent testing, possibly resulting in safer patient outcomes, further dosage optimization, and increased compliance. This article presents a device that measures the s-lithium concentration from whole blood. The device consists of a single-use cartridge able to conduct on-chip serum filtration, volume-metering and an on-chip colorimetric assay. Spiked whole blood shows good linearity (Pearson's $r = 0.96$, $R^2 = 0.92$), a limit-of-detection of 0.3 mmol L^{-1}, and an average deviation of 0.05 mmol L^{-1} ($\pm 6\%$) compared to atomic absorption spectroscopy. The on-chip colorimetric assay has shown to be a promising technique for measuring s-lithium concentration from whole blood and could allow patients to assess lithium levels at home and make the treatment available for new patient groups.

Introduction

Bipolar disorder is a severe disorder affecting 1–2% of the population.[1] Patients with bipolar disorder experience severe mood swings and can veer between states of mania and depression. These mood swings drastically impair the patient's quality of life and are associated with an increased risk of self-harm and suicide.[2] Lithium is one of the most effective treatments for bipolar disorder, and its use in modern treatment can be traced to the early 1960s.[3] However, the therapeutic window of serum (s-)lithium is narrow (0.4–1.2 mmol L^{-1}) and near the toxicity range (>1.5 mmol L^{-1}),

[a] *Micro and Nanosystems, School of Electrical Engineering and Computer Science, KTH Royal Institute of Technology, Stockholm, Sweden. E-mail: roxhed@kth.se*
[b] *Department of Molecular Medicine and Surgery, Karolinska Institutet, Stockholm, Sweden*
[c] *Psychiatry Southwest, Stockholm Healthcare Services, Stockholm, Sweden*
[d] *Centre for Molecular Medicine, Karolinska University Hospital, Stockholm, Sweden*
[e] *Division of Biomolecular and Cellular Medicine, Department of Laboratory Medicine, Karolinska Institutet, Stockholm, Sweden*
[f] *Department of Cellular Therapy and Allogeneic Stem Cell Transplantation (CAST), Karolinska University Hospital, Huddinge, Sweden*
[g] *Karolinska ATMP Center, ANA Futura, Huddinge, Sweden*
[h] *Department of Clinical Neuroscience, Karolinska Institutet, Stockholm, Sweden*
[i] *MedTechLabs, BioClinicum, Karolinska University Hospital, Solna, Sweden*

necessitating continuous therapeutic drug monitoring during lithium treatment to prevent adverse effects.[4] Patients are typically monitored weekly at the start of the treatment and, after the levels have stabilized within the target range, follow-ups are performed once every three-to-six months. This involves regular hospital visits for venous blood sampling, which is cumbersome for patients and consumes healthcare resources. For a patient being treated with lithium, this process is continuous and lifelong. Therapeutic drug monitoring in hospitals also requires facilities to analyze the samples; patients living in areas without the necessary infrastructure are limited to other medications or could be put at higher risk during treatment.[5] Even in areas with necessary infrastructure and established guidelines, laboratory monitoring has been shown to be suboptimal.[6] Another factor increasing patient risk is treatment nonadherence. For example, it has been reported that 54% of patients in a study discontinued their treatment during the study window.[7] The main reasons for discontinuing treatment were adverse effects (62%), such as diarrhea and tremors, followed by psychiatric effects (44%), with one of the psychiatric effects being fear of adverse effects. These adverse effects could be addressed with a simple dose adjustment. Hence, improved routines for continuous therapeutic drug monitoring of lithium are urgently needed.

A way to reduce discontinuation rates would be to increase the testing frequency by moving toward patient-centric testing. Medical devices for decentralized on-demand home

testing would allow more frequent monitoring and thus help patients make informed decisions regarding their lithium treatment.[5] One example is the use of devices for self-sampling in the form of dried blood spots or dried plasma spots. Such devices are simple and can be sent to centralized labs for analysis, providing highly accurate results.[8,9] However, the lag time between sampling and results in the patient feedback loop limits the value and effectiveness of such an approach, even if it could be cost-effective.[10] A better alternative would be to combine capillary blood sampling and analyte quantification in a point-of-care (POC) sensor, which could be used by untrained patients.[10] Such a device would allow increased testing frequency and enable more rapid responses to deviations in the patient's s-lithium levels.

Lithium concentrations can be measured in several ways.[10] Optical methods such as fluorometric,[11,12] and colorimetric assays,[13–15] including porphyrin assays,[16,17] have been proposed and developed into commercial assays for laboratory use alongside gold standard methods such as atomic absorption spectroscopy (AAS).[18] Recently, there has been a push to establish ion-selective electrode methods for whole blood,[19] serum,[20,21] and sweat.[22–24] Another promising approach is capillary electrophoresis.[25–27] Floris *et al.* developed an electrophoresis-based POC device for blood sample analysis using disposable glass chips; the device was later commercialized under the brand name Medimate.[28,29] In this approach, the manufacturing of the tailor-made glass chips was reported as the cost-determining part of the product, limiting its potential use as a cost-effective disposable device.[28] To obtain a cost-effective solution, Komatsu *et al.* developed a paper-based device for measuring plasma lithium levels combined with image analysis for the colorimetric readout and developed a digital microfluidic system to load samples into the sensor paper.[30,31] However, further evaluation would be necessary to demonstrate clinical translatability of this approach due to the use of diluted blood, as well as the lack of evaluation of hematocrit-independence and storage stability in the published study. Hence, there is still a need for complete, low-cost, clinically relevant solutions incorporating sample preparation.

Here we present a cost-effective and patient-centric device able to measure the s-lithium concentration directly from capillary finger-prick blood. The device combines on-chip serum filtration and volume-metering technology, which have previously reported a CV of 3% in volume variation,[32] with a colorimetric assay for on-chip colorimetric readout. The developed concept can potentially enable low-cost POC s-lithium measurement for frequent self-monitoring, which could lead to safer and more effective treatment of patients affected by bipolar disorder.

Experimental

Device operational principle and design

The device consists of a plastic disposable microfluidic cartridge designed to process two drops of blood (50–100

μL) and, after pushing a reagent blister pack, provide quantitative information regarding the s-lithium concentration in the sample (Fig. 1). An overview of the process is illustrated in Fig. 1A.

After adding blood, typically from a finger-prick, at the inlet of the cartridge, the sample is automatically filtered by capillary action to obtain blood serum, the volume of which is then subsequently metered in a microchannel. Upon injection of the reagent stored in the blister pack on the cartridge, the serum is mixed with reagent by inverting the cartridge, end over end, ten times. Following a 10 minute wait period, as specified in the manufacturer's instructions, during which the colorimetric reaction takes place. The reaction produces a change in color proportional to the s-lithium concentration. The cartridge is portable, simple to use, and provides quick results that are available to the patient within 30 minutes.

The cartridge, shown in Fig. 1B, consists of four main parts: a sample-inlet area, a reagent blister pack, a readout chamber, and a microfluidic chip network connecting the former three. The blister pack contains a colorimetric reagent that absorbs different amounts of light at specific wavelengths depending on the amount of lithium binding to it (Fig. 1C). To use the device, at least 50 μL of whole blood is applied to the sample-inlet area. When blood touches the sample-inlet area, serum is filtered out from the sample by a blood separation filter arranged in a wedge configuration (Fig. 1D, steps I and II).[33] Extracting the serum from whole blood removes interference from hemoglobin in the final readout process. The separated serum then enters a microfluidic channel and is volumetrically metered (Fig. 1D, step III) as previously described.[32] The separation and volume-metering processes take between 5 and 15 minutes after sample application, after which the colorimetric reagent is introduced into the microfluidic cartridge by pressing the blister. Bubble formation caused by surfactants in the commercially available reagent can interfere with the readout, and thus, a debubbler network is introduced to remove bubbles formed by the injection of the reagent. The bubble-free reagent then pushes the serum into the readout chamber (Fig. 1D, step IV). After filling the readout chamber, the sample and reagent are mixed and left for 10 minutes to ensure consistent color change (Fig. 1D, step V). Finally, the lithium concentration can be visually estimated or measured using a spectrophotometer (Fig. 1D, step VI). An example of the color change is shown in the inset of Fig. 1B.

Materials and methods

As illustrated in Fig. 2, the device consists of eight layers of tapes [adhesive tape 1 (64620, Tesa, Sikab, Sweden, thickness 170 μm) and adhesive tape 2 (8132LE, 3M, Digi-key, thickness 50 μm)], five layers of hydrophilic plastic sheets (3R3028 Xerox Type C, Elmsok, UK, thickness 100 μm), ten pieces of chromatography paper (Ahlstrom-Munksjö FN100, VWR, Sweden, thickness 300 μm), a layer of 2 mm PMMA (Crylux
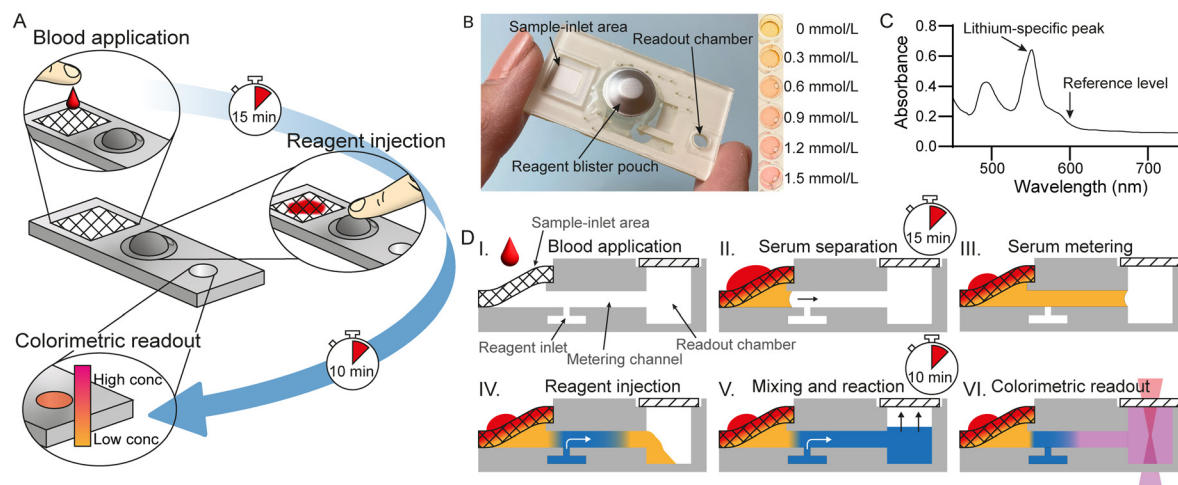
Fig. 1 A) Overview of the device usage concept. B) Image of the device cartridge, 50 × 27 × 3.5 mm in size, with the main components indicated. The inset shows pictures of example colorimetric results at different concentrations with backlighting (1 : 20 sample to reagent ratio). C) An absorption curve at 0.9 mmol L^{-1} with the lithium associated color specific peak (546 nm) and reference level (600 nm). D) The working principle of the device (cross-section) shows blood application (I), serum separation (II), metering (III), reagent injection (IV), mixing and reaction (V), and readout procedure (VI).

clear 1000, 3A composites GmbH, Germany), a blood filter membrane (SG regular, IPOC, Canada), a porous membrane (ipPore 1000M10/620M100/A4, it4ip, Belgium), and a blister pack (custom blister pouches 150 μL, Microfluidic ChipShop, Germany) filled with a commercial colorimetric lithium reagent (ESPA Li II, NIPRO Co. Inc., Japan). A 3D printed blister adapter from a Form 3 + 3D printer (clear V4 resin, Formlabs, USA) was glued to the device using adhesive tape 2 and epoxy (Power Epoxy Extra Time, Loctite, Clas Ohlsson, Sweden).

Whole blood samples were obtained from blood donors (Blodcentralen, Stockholm, Sweden) in BD Vacutainer citrate tubes. 2 M lithium sulfate solution, corresponding to 4 M of lithium, was purchased from Merck (Sweden), NIST lithium standard solution (9.969 ± 0.030 mg g^{-1}) and sodium chloride (NaCl) were from Sigma-Aldrich (Sweden), and phosphate-buffered saline (PBS) tablets were from PanReacAppliChem (1 L, pH 7.4, VWR, Sweden) mixed with deionized water (Milli-Q® Type I, Merck, Sweden).

All experiments were performed in accordance with the guidelines for care of the Swedish legislation, and experiments were approved by the Swedish Ethical Review Authority (Dnr. 2021-04164). Informed consents were obtained from human participants of this study.

Device fabrication. Devices were fabricated using lamination technology, as previously described,[32,33] according to the schematic illustration in Fig. 2. Using a CO_2 laser cutter (VLS 2.3, Universal Laser Systems, Austria), individual layers of PMMA, adhesive tape, and hydrophilic sheets were structured to create flow paths. The porous membrane was cut into 7 × 7 mm^2 using scissors. The edges of the blood filter were cut into 10 × 10 mm^2 squares, and the edges were submerged into liquified wax (Cartridge-Free ColorQube® Ink, Xerox, USA) to prevent blood cell leakage, as previously described.[32]

Blood sample preparation and device use. Ten whole blood samples were analyzed using a hematology analyzer (Swelab Alfa, Boule Medical AB, Sweden) to determine all samples' hematocrit (HCT). HCT is the fraction of red blood cells and needs to be considered when spiking blood since it affects the final lithium concentration in the sample. All ten blood samples were split into two, and fifteen of the split samples were spiked with a lithium sulfate solution consisting of PBS to a 1 : 100 of an HCT-corrected estimated final whole blood concentration between 0 mmol L^{-1} and 1.5 mmol L^{-1}. Spiked whole blood will not have the same lithium concentration as the sample, and therefore, the lithium concentration was determined using AAS. The samples were then mixed using an IKA Loopster digital rotating mixer (IKA Works GmbH & Co, Germany) at 15 rpm for one hour. A randomly assigned volume between 50 μL and 100 μL (increments of 10 μL) of spiked blood was added to each device. The blister was pressed 15 minutes after sample addition to ensure that the sample had filled the channel. After another 10 minutes, the absorption was measured using a SpectraMax 340PC (Molecular Devices, USA) at 546 nm and 600 nm. A 96-well plate (734-2781, VWR, Sweden) was laser cut as a holder for the cartridge and used during the absorption measurements.

Atomic absorption spectroscopy. All spiked blood samples were centrifuged at 2000g for 10 min, and the plasma was collected. A common calibration sample was prepared using a certified NIST reference standard solution to compare the device to AAS.[18] Calibration samples were prepared following the NIST instructions to prepare standards by mass with concentrations ranging from 0 mmol L^{-1} to 2 mmol L^{-1}.

10 μl of centrifuged blood plasma or calibration samples were added to 290 μl of 0.56 mmol L^{-1} NaCl. AAS analysis was performed using a Thermo iCE 3000 AA spectrometer
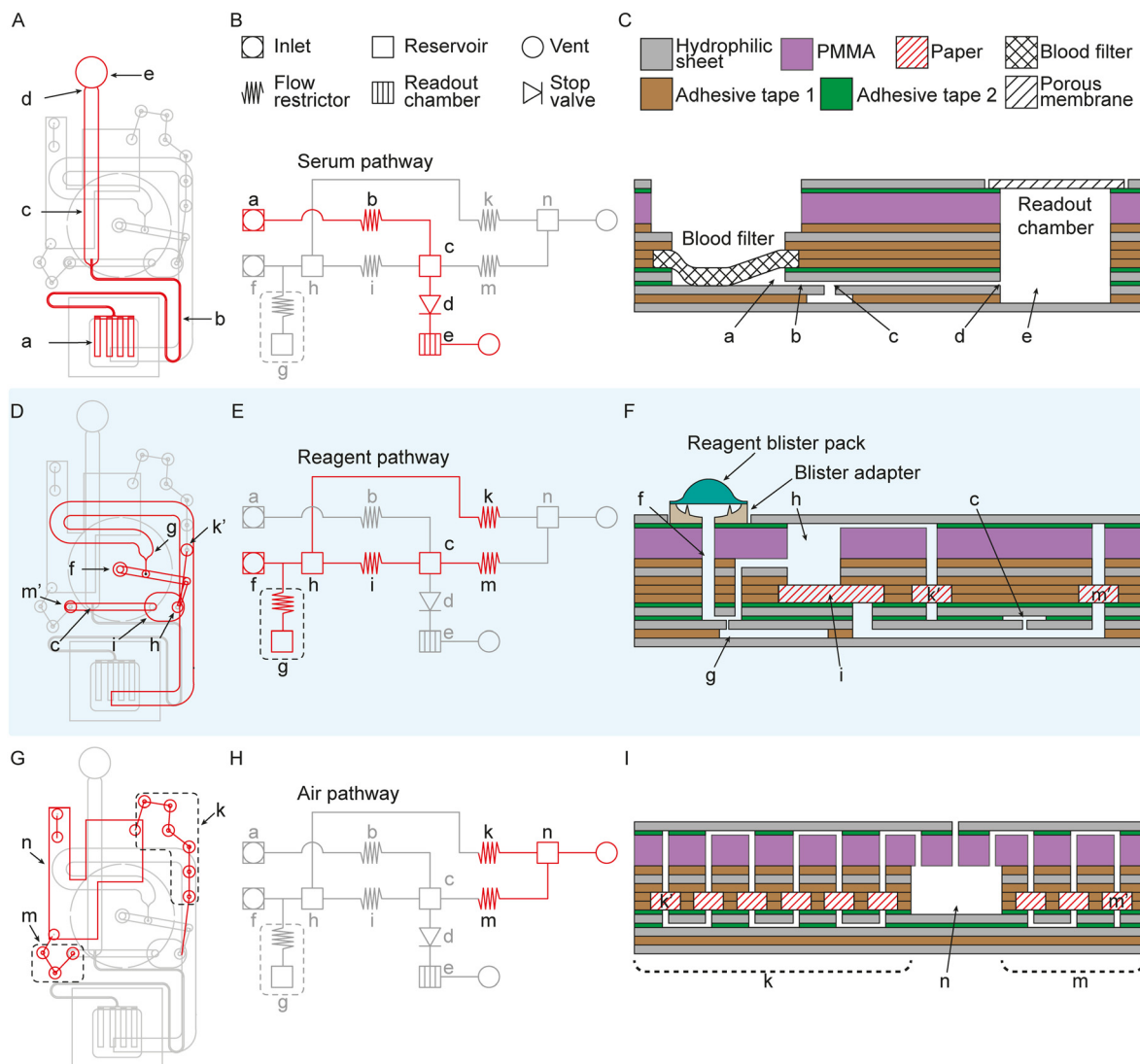
Fig. 2 A) Schematic illustration of the device cartridge with the pathway between the serum inlet (a), flow restrictor (b), metering channel (c), stop valve (d), and readout chamber (e) highlighted. Scale 1 : 1. B) Symbolic illustration of the device cartridge with the pathway between the serum inlet (a), flow restrictor (b), metering channel (c), stop valve (d), and readout chamber (e) highlighted. C) The cross-sectional illustration of the cartridge with the blood filter, readout chamber (e), serum inlet (a), flow restrictor (b), metering channel (c), stop valve (d), and readout chamber (e) marked. D) Schematic illustration of the device cartridge with the reagent pathway between the reagent inlet (f), pressure buffer (g), debubbeling reservoir (h), debubbeling flow restrictor (i), metering channel (c), and the first vent flow restrictors (k′ and m′) highlighted. Scale 1 : 1. E) Symbolic illustration of the device cartridge with the reagent pathway between the reagent inlet (f), pressure buffer (g), debubbeling reservoir (h), debubbeling flow restrictor (i), metering channel (c), and the vent flow restrictors (k and m) highlighted. F) The cross-sectional illustration of the device cartridge with the reagent blister pack, blister adapter, and the reagent pathway between the reagent inlet (f), pressure buffer (g), debubbeling reservoir (h), debubbeling flow restrictor (i), metering channel (c), and the first vent flow restrictors (k′ and m′) marked. G) Schematic illustration of the device cartridge with the vent flow restrictors (k and m) and the waste reservoir (n) highlighted. Scale 1 : 1. H) Symbolic illustration of the device cartridge with the vent flow restrictors (k and m) and the waste reservoir (n) highlighted. I) The cross-sectional illustration of the device cartridge with the first (k′ and m′) and following (k and m) vent flow restrictors together with the waste reservoir (n) marked.

(Thermo Fisher Scientific, USA) with a 100 mm burner and 0.4 mm sample inlet. The instrument was used in flame ionization mode, and absorption was measured at 670.8 nm with a measurement time of 8 s and a bypass setting of 0.5 nm using transient area mode. The AAS was operated with Termo Solaar software v.11.11.

Reagent kinetics. Lithium sulfate samples ranging from 0 mmol L^{-1} to 1.5 mmol L^{-1} were added to a 96-well plate, and reagent (1 : 20, sample to reagent) was added to the each well.

The plate was then immediately and continuously measured every 10 seconds for 12 minutes using a SpectraMax 340PC at 546 nm and 600 nm.

Evaporation measurement. We verified the evaporation rate over the porous membrane using devices with only the reaction chamber with the porous membrane. The readout chambers were filled with reagent and the reagent inlet was sealed to facilitate reagent loss only from the readout chamber. The device was put on a AT261 DeltaRange scale

(Mettler Toledo, USA) and its weight was recorded every minute for 15 min. The scale was in an open configuration to simulate normal room conditions.

Flow cytometry assay. To investigate the platelet content in the filtrate, blood samples from five different individuals were centrifuged to obtain plasma or filtrated, to obtain filtrate by passing whole blood through the blood filter using a previously described device.[33] Platelet-related surface markers on extracellular vesicles (EVs) contained in respective samples (CD9, CD41b, CD42a, CD62P) were assessed using multiplex bead-based EV flow cytometry (MACSPlex EV Kit IO, Miltenyi Biotec) as previously described.[34] Samples were diluted with MACSPlex buffer to a final volume of 60 μL and incubated over-night with 10 μL MACSPlex exosome capture beads on an orbital shaker at room temperature in the dark. Beads were washed with MACSPlex buffer, and then 4 μL of APC-conjugated CD9, CD63, and CD81 detection antibodies were added to each sample in a total volume of 135 μL to facilitate EV detection. After incubation for 1 hour on an orbital shaker at room temperature, samples were washed and incubated for another 15 minutes before a final washing step was performed. Incubation and washing steps were performed in 0.22 μm filter plates. Final samples were resuspended in 150 μL MACSPlex buffer and acquired on a MACSQuant Analyzer 16 flow cytometer (Miltenyi Biotec). Data was analyzed with FlowJo software version 10.9.0 and expressed as log10-transformed fold change values over respective non-EV containing buffer controls as described before.[35] A heatmap was generated with Morpheus (**https://software.broadinstitute.org/morpheus**) and is presented in Fig. 3. As shown in Fig. 3, the approach with filtrating the blood sample to obtain filtrate results in a removal of platelet markers in the filtrate, making it more serum-like even in a citrate treated blood sample. For this reason, we use the name "serum" for all operational descriptions of the device

since it is intended to be used with finger-prick blood without anticoagulants, while method descriptions use "sample" to avoid confusion with the filtrate sample type.

Results and discussion

Detailed step-by-step device operation

Fig. 2 illustrates the different parts of the device: serum separation and metering (Fig. 2A–C), bubble remover (Fig. 2D–F), and the air pathway (Fig. 2G–I). Due to the complexity of the device, all dimensions are given in a 1:1 vector file format with the thickness of each layer marked. This file (Li device print files.ai) is available in the Zenodo repository (**https://doi.org/10.5281/zenodo.15000292**).

Serum filtration starts by applying 50–100 μL whole blood to the sample-inlet area. The sample inlet area consists of a blood separation filter, separating the red blood cells from the serum. The filter is attached to a hydrophilic sheet to facilitate autonomous capillary filtration. When the serum has been filtered out, it enters the inlet (a), moving through the flow restrictor (b [65 mm × 0.4 mm × 0.05 mm]), filling the metering channel (c [25 mm × 2 mm × 0.05 mm]) before being stopped by a geometric stop valve (d).[36] This process takes approximately 15 minutes. The flow restrictor (b) prevents backflow into the inlet (a) and is a part of the pressure buffer (g). The reagent is introduced by pressing on top of the blister pack when the metering channel (c) has been filled with 2.5 μL.

The reagent enters the microfluidic chip through a second inlet (f). There is a blister adapter in between the blister and the microfluidic chip. The blister adapter is designed to break the blister when force is applied to the blister by the operator and guide the flow into the reagent inlet (f). It is also designed to let as much air out as possible under the blister to reduce the bubble formation by surfactants in the reagent so as not to overload the debubbler. The reagent is forced to pass through a debubbler to eliminate the remaining bubbles. The debubbler consists of a pressure buffer (g [70 mm × 2 mm × 0.05 mm]) and a reservoir (h [diameter 1.5 mm, height 2.49 mm]), connected to two flow resistors, one for venting out air with a high flow resistance (k) and one with a lower flow resistance for slowing down the flow speed and blocking bubbles (i [approximately a 5.7 mm × 4.2 mm square with fully rounded edges along the short side of the paper mesh, FN100 paper]) from continuing to the metering channel (c). As the reservoir (h) fills up with reagent and bubbles enter the reservoir, the paper in the flow restrictor (i) slows down the flow and gives time for the bubbles to rise, leaving a bubble-free portion at the bottom of the reservoir. The paper in the flow restrictor (i) also acts as a mesh filter, blocking bubbles from moving past the flow restrictor (i) and into the metering channel (c). The channel in between the flow restrictor (i) and metering channel (c) is vented through a high resistance flow restrictor (m) to not trap air and ensure a bubble-free flow to the metering channel (c). The reagent pushes the sample through the
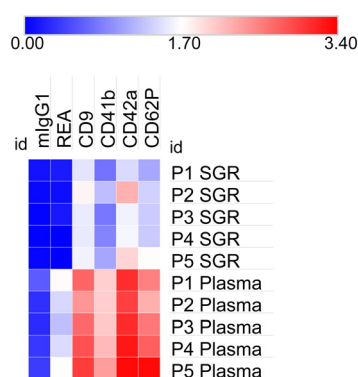
Fig. 3 Heatmap comparing the concentrations of platelet markers CD9, CD41b CD42a and CD62P in filtrate from the blood filter SG regular (SGR) with centrifugated plasma from five different individuals (P1–P5). Values are expressed as log10-transformed fold change. There is a clear decrease of platelet markers in the filtrate compared to the plasma samples. mIgG1 and REA are non-EV containing buffer controls.

metering channel (c) and into the readout chamber (e [diameter 4.5 mm, height 3.3 mm]), where the volume is geometry defined to a 1 : 20 v/v ratio between the sample and reagent. The readout chamber is vented through a transparent porous membrane.

The pressure buffer (g) consists of a dead-end microfluidic channel with a small flow restrictor at the inlet. When force is applied to the blister pack, the air in the channel is compressed by the liquid, effectively storing liquid in the microfluidic channel. When the force is removed from the blister pack, a negative pressure is created, pulling a small amount of liquid back towards the blister. The compressed air in the pressure buffer pushes the reagent back into the microfluidic network, effectively compensating for the negative pressure and preventing the negative pressure from introducing bubbles into the microfluidic network. The two high-resistance flow restrictors (k and m) redirect flow away from air vents and towards the readout chamber, minimizing through vents. The reagent loss through the vents is collected in a waste reservoir (n) to keep the reagent contained in the cartridge.

Performance

To evaluate the device performance, we analyzed spiked venous whole blood samples from ten healthy human donors using different lithium concentrations. The spiked blood samples were added to 33 devices at different volumes ranging from 50–100 μL to simulate a capillary finger-prick sample of two to three drops of blood. 25 (76%) of 33 devices operated successfully from sample addition to readout. The results obtained with the device were compared to gold-standard AAS to obtain the sample concentration and a calibration curve, reported in Fig. 4A. The limit-of-detection (LOD) from the calibration curve was 0.3 mmol L^{-1}, allowing the device to cover the entire physiological therapeutic concentration range (0.4–1.2 mmol L^{-1}). To evaluate the accuracy of the device, the s-lithium concentration in spiked blood was compared to the actual sample concentration determined by AAS and the

results are presented in Fig. 4B. Fig. 4B shows a Passing Bablok regression with good linearity with a Pearson's r of 0.96 ($R^2 = 0.92$) and a unitless slope of 0.98. The accuracy of the device-determined values is sufficient to estimate the s-lithium concentration over the entire physiological therapeutic concentration range. Most devices had a deviation below 0.1 mmol L^{-1}, as shown in the Bland–Altman plot in Fig. 4C. The average absolute deviation of 0.05 mmol L^{-1} (equal to 6%) suggests that the presented concept could be used to determine the s-lithium concentration in blood with adequate sensitivity and reproducibility to be clinically relevant. The results demonstrate that the device offers similar accuracy (approximately 0.1 mmol L^{-1}) to other devices.[19,26,30]

Eight tested devices were removed because of bubbles introduced during the serum-filling procedure or in the readout chamber caused by reagent blister leakage. This together with the increased spread seen in the Bland–Altman plot (Fig. 4C), at higher concentrations, could be attributed to misalignments from the manual assembly of the devices. Reducing or eliminating defects during device assembly is expected to eliminate such occasional issues and improve the accuracy and precision of the device.

To ensure that the evaporation over the porous membrane does not influence the lithium concentration in the readout chamber, the evaporation rate over the membrane was studied. It was observed that the evaporation rate over the porous membrane is more or less constant between devices, see ESI† Fig. S1. Any reagent loss from evaporation is backfilled with excess reagent stored in the device, keeping the volume in the readout chamber constant and consistent during the reaction time, see ESI† Fig. S2, and between devices. Even if the theoretical volume loss during the 10 minute reaction time for the reagent would be around 4% (around 2 μL), there is currently no reason to believe this is the cause for any variations.

While the current assay takes 25 to 30 minutes, there are possibilities to shorten the assay time. The time for sample filtration and metering is the most time-consuming part of
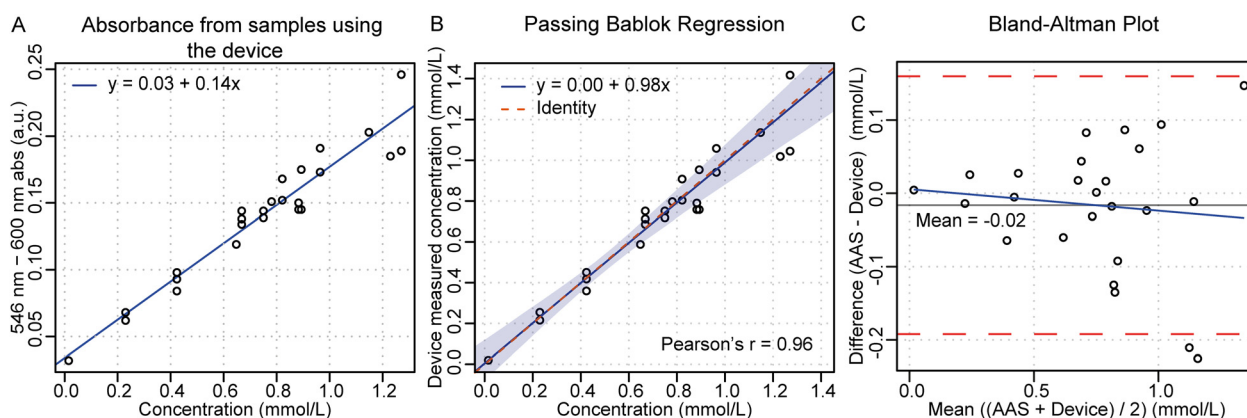
Fig. 4 A) Calibration plot comparing the absorbance from 25 devices, with lithium spiked blood, and the sample concentration. B) Passing Bablok regression plot with a 95% confidence interval comparing the device measured concentration to the sample concentration determined by AAS. C) Bland–Altman plot comparing the absolute difference between the device determined concentration and the sample concentration.

the assay and we believe that a more automated assembly process of the device could reduce the filtration time to around 5 minutes. Currently, most devices take less than 5 minutes to complete the sample filtration and metering process. However, the current 15 minute sample filtration and metering time limit is set to capture outliers, which takes longer to fill. Improving manufacturing precision and reducing variations between devices will most likely improve the sample filtration and metering time consistency to less than 5 minutes. Another possible way to reduce the assay time would be to shorten the time to color change. The manufacturer protocol stipulates 10 minute waiting time; however, equilibrium for the therapeutic window (up to 1.2 mmol L^{-1}) is reached before 10 minutes, see ESI† Fig. S3. It could be feasible to perform the measurement 1–2 minutes earlier without compromising results. Additional time optimizations could potentially come from modifications of the reagent or improved mixing. Hence, by combining reagent improvements with reduced sample filtration and metering time, it may be possible to decrease the total assay time to around 10–13 minutes. However, as shown in Fig. S3,† the reagent chemistry does require some time. Changes to the chemical composition of the reagent could allow for faster reactions, but this would require further investigations.

In the future, this concept would benefit from a dedicated device reader, which could be kept at home. Handheld colorimetric readers (for example, water alkali ion meters) trade at around 100–500 USD and provide sufficient resolution and accuracy for ion concentration measurements similar to the ranges required for the presented device. We believe that the same technology could be used for our device. Scientific literature includes examples where the cost of goods is approximately 20 USD (ref. 37) and makes us confident that a relatively low-cost dedicated reader using currently available technologies would be feasible.

A POC home test for s-lithium in blood could allow for patient-centric testing of s-lithium, possibly allowing for an increased testing frequency and improving the treatment safety. Giving results directly to the patient would reduce the testing burden on the healthcare system, improving the health and life quality of existing patients while also expanding access of lithium treatment to new patient groups in developing countries and other areas where the necessary infrastructure is lacking today.

Conclusions

Therapeutic drug monitoring is essential for patients undergoing lithium-based treatment. There is thus a need for decentralized patient-centric POC tests for s-lithium in blood, enabling more frequent on-demand testing. In this study, we evaluate a device using an on-chip colorimetric assay to measure s-lithium concentrations starting from capillary whole blood. The device demonstrated similar accuracy to previous devices for whole-blood samples analysis in the medically relevant concentration range, with a Pearson's r of 0.96 and an average absolute deviation of 0.05 mmol L^{-1}, or ±6%.

The presented device, built with low-cost materials, shows that on-chip serum filtration and volume-metering, combined with an on-chip colorimetric readout, is a promising technique for measuring s-lithium concentration in blood. Our results indicate the device potentially has clinical relevance and could allow for patient-centric testing of s-lithium in blood, allowing patients to take samples at home or at the POC. The use of such a device could thus reduce the need for the patient to conduct regular hospital visits for venous blood sampling.

We expect that further optimizations in cartridge manufacturing will improve the accuracy and precision of the device while enhancing reliability and robustness. Further evaluations using patient samples are required to demonstrate robust and reproducible performance in clinical samples, including the direct application of finger-prick blood without anticoagulants. POC use performed by minimally trained operators would also have to be shown and would require the development of a dedicated reader to analyze the sample. However, we are comfortable that the development of such a dedicated reader is possible with the currently available technologies.

A POC home test for s-lithium levels in blood could make the treatment more readily available and enable the use of lithium for new patients living in areas without the necessary infrastructure. It would also give patients the ability to get on-demand results without the need for hospital visits and give the opportunity to increase testing frequency, which would increase the safety, compliance, and availability of the treatment.

Data availability

All data, R code, schematics, and print files are available in the main text, ESI,† or available in the Zenodo repository at https://doi.org/10.5281/zenodo.15000292.

Author contributions

Conceptualization, C. O., J. H., F. R., M. S., L. B., and N. R.; methodology, C. O., J. H., F. R., O. B., and N. R.; investigation, C. O., J. H., F. R. and A. G.; visualization, C. O.; funding acquisition, L. B., and N. R.; project administration, F. W., L. B., and N. R.; supervision, M. S., L. B., and N. R.; writing – original draft, C. O.; writing – review & editing, all authors.

Conflicts of interest

C. O., J. H., F. R., M. S., L. B., and N. R. have submitted a patent application (PCT/EP2024/078419) describing the materials and applications of the systems described here. Other authors declare no conflicts of interest.

Acknowledgements

Notes and references

1 S. Pini, V. De Queiroz, D. Pagnin, L. Pezawas, J. Angst, G. B. Cassano and H. U. Wittchen, *Eur. Neuropsychopharmacol.*, 2005, **15**, 425–434.

2 I. M. Anderson, P. M. Haddad and J. Scott, *Br. Med. J.*, 2013, **346**(7889), 27–32.

3 E. Shorter, *Bipolar Disord.*, 2009, **11**, 4–9.

4 J. S. Kang and M. H. Lee, *Korean J. Intern. Med.*, 2009, **24**(1), 1–10.

5 U. Mannapperuma, P. Galappatthy, R. L. Jayakody, J. Mendis, V. A. De Silva and R. Hanwella, *BMC Psychiatry*, 2019, **19**(1), 194.

6 A. Bosi, L. Ceriani, C. G. Elinder, R. Bellocco, C. M. Clase, M. Landen, J. J. Carrero and B. Runesson, *Bipolar Disord.*, 2023, **25**, 499–506.

7 L. Öhlund, M. Ott, S. Oja, M. Bergqvist, R. Lundqvist, M. Sandlund, E. Salander Renberg and U. Werneke, *BMC Psychiatry*, 2018, **18**(1), 37.

8 I. D. Manfro, M. Tegner, M. E. Krutzmann, A. do C. Artmann, M. R. Brandeburski, G. P. Peteffi, R. Linden and M. V. Antunes, *Talanta*, 2020, **216**, 120907.

9 F. Wikström, C. Olsson, B. Palm, N. Roxhed, L. Backlund, M. Schalling and O. Beck, *J. Pharm. Biomed. Anal.*, 2023, **227**, 115269.

10 M. Sheikh, M. Qassem, I. F. Triantis and P. A. Kyriacou, *Sensors*, 2022, **22**(3), 736.

11 J. H. Kim, D. Diamond and K. T. Lau, *Development of Non-invasive Biochemical Device for Monitoring the Lithium Level from Saliva for Bipolar Disorder Patients*, IEEE, 2011.

12 T. Gunnlaugsson, B. Bichell and C. Nolan, *Tetrahedron Lett.*, 2002, **43**(28), 4989–4992.

13 J. K. Trautman, V. P. Y. Gadzekpo and G. D. Christian, *Talanta*, 1983, **30**(8), 587–591.

14 D. Gruson, A. Lallali, V. Furlan, A. M. Taburet, A. Legrand and M. Conti, *Clin. Chem. Lab. Med.*, 2004, **42**, 1066–1068.

15 M. Iwai, F. Kondo, T. Suzuki, T. Ogawa and H. Seno, *Leg. Med.*, 2021, **49**, 101834.

16 M. Tabata, J. Nishimoto and T. Kusano, *Talanta*, 1998, **46**(4), 703–709.

17 B. Rumbelow and M. Peake, *Ann. Clin. Biochem.*, 2001, **38**(6), 684–686.

18 E. L. Garner, L. A. Machlan, J. Mandel, R. C. Paule, T. C. Rains and R. A. Velapoldi, *Standard Reference Materials*, MD, Gaithersburg, 1980.

19 M. Novell, T. Guinovart, P. Blondeau, F. X. Rius and F. J. Andrade, *Lab Chip*, 2014, **14**, 1308–1314.

20 R. L. Bertholf, M. G. Savory, K. H. Winborne, J. C. Hundley, G. M. Plummer and J. Savory, *Clin. Chem.*, 1988, **34**(7), 1500–1502.

21 F. Coldur and M. Andac, *Electroanalysis*, 2013, **25**, 732–740.

22 F. Criscuolo, I. Ny Hanitra, S. Aiassa, I. Taurino, N. Oliva, S. Carrara and G. De Micheli, *Sens. Actuators, B*, 2021, **328**, 129017.

23 F. Criscuolo, I. Taurino, F. Stradolini, S. Carrara and G. De Micheli, *Anal. Chim. Acta*, 2018, **1027**, 22–32.

24 F. Criscuolo, I. Taurino, S. Carrara and G. De Micheli, *A novel electrochemical sensor for non-invasive monitoring of lithium levels in mood disorders*, 2018.

25 E. X. Vrouwe, R. Luttge and A. van den Berg, *Electrophoresis*, 2004, **25**, 1660–1667.

26 E. X. Vrouwe, R. Luttge, W. Olthuis and A. van den Berg, *Electrophoresis*, 2005, **26**, 3032–3042.

27 E. X. Vrouwe, R. Luttge, I. Vermes and A. Van Den Berg, *Clin. Chem.*, 2007, **53**, 117–123.

28 A. Floris, S. Staal, S. Lenk, E. Staijen, D. Kohlheyer, J. Eijkel and A. Van Den Berg, *Lab Chip*, 2010, **10**, 1799–1806.

29 S. Staal, M. Ungerer, A. Floris, H. W. Ten Brinke, R. Helmhout, M. Tellegen, K. Janssen, E. Karstens, C. van Arragon, S. Lenk, E. Staijen, J. Bartholomew, H. Krabbe, K. Movig, P. Dubský, A. van den Berg and J. Eijkel, *Electrophoresis*, 2015, **36**(5), 712–721.

30 T. Komatsu, M. Maeki, A. Ishida, H. Tani and M. Tokeshi, *ACS Sens.*, 2020, **5**, 1287–1294.

31 T. Komatsu, M. Tokeshi and S. K. Fan, *Biosens. Bioelectron.*, 2022, **195**, 113631.

32 J. Hauser, G. Lenk, S. Ullah, O. Beck, G. Stemme and N. Roxhed, *Anal. Chem.*, 2019, **91**, 7125–7130.

33 J. Hauser, G. Lenk, J. Hansson, O. Beck, G. Stemme and N. Roxhed, *Anal. Chem.*, 2018, **90**, 13393–13399.

34 O. P. B. Wiklander, R. B. Bostancioglu, J. A. Welsh, A. M. Zickler, F. Murke, G. Corso, U. Felldin, D. W. Hagey, B. Evertsson, X.-M. Liang, M. O. Gustafsson, D. K. Mohammad, C. Wiek, H. Hanenberg, M. Bremer, D. Gupta, M. Björnstedt, B. Giebel, J. Z. Nordin, J. C. Jones, S. EL Andaloussi and A. Görgens, *Front. Immunol.*, 2018, **9**, DOI: **10.3389/fimmu.2018.01326**.

35 V. V. T. Nguyen, J. A. Welsh, T. Tertel, A. Choo, S. I. van de Wakker, K. A. Y. Defourny, B. Giebel, P. Vader, J. Padmanabhan, S. K. Lim, E. N. M. Nolte-'t Hoen, M. C. Verhaar, R. B. Bostancioglu, A. M. Zickler, J. M. Hong, J. C. Jones, S. EL Andaloussi, B. W. M. van Balkom and A. Görgens, *J. Extracell. Vesicles*, 2024, **13**(6), e12463.

36 P. F. Man, C. H. Mastrangelo, M. A. Burns and D. T. Burke, Microfabricated capillarity-driven stop valve and sample injector, in *Proceedings MEMS 98. IEEE. Eleventh Annual International Workshop on Micro Electro Mechanical Systems. An Investigation of Micro Structures, Sensors, Actuators, Machines and Systems (Cat. No.98CH36176*, IEEE, Heidelberg, Germany, 1998, pp. 45–50, DOI: **10.1109/MEMSYS.1998.659727**.

37 W. Tang, M. Zhang, T. Yue, X. Wang and Z. Li, *Sens. Actuators, B*, 2021, **346**, 130523.